Supporting Information (SI)

Photophysical and thermodynamic delineation of binding interaction of anticancer alkaloid chelerythrine towards triplex and duplex DNA structures: a comparative approach

Rapti Goswami, Himal Das[#], Lopa Paul[#], Amar Ghosh, Susmita Chowdhury, Ribhu Banerjee and Suman Das*

Biophysical Chemistry Laboratory, Physical Chemistry Section, Department of Chemistry, Jadavpur University, Raja S. C. Mullick Road, Jadavpur, Kolkata 700032, India

[#] Equal contribution each

*Corresponding Author:

Suman Das

E-mail: sumandas10@yahoo.com (S. Das)

Tel.: +91 94 3437 3164, +91033 2457 2349

Fax: +91 33 2414 6266

E-mail addresses: raptirai6@gmail.com (R. Goswami), himaldas2021@gmail.com (H. Das), lopapaul6@gmail.com (L. Paul), amar.off2233@gmail.com (A. Ghosh), chowdhurysusmita72@gmail.com (S. Chowdhury), ribhubanerjee.wb@gmail.com (R. Banerjee)

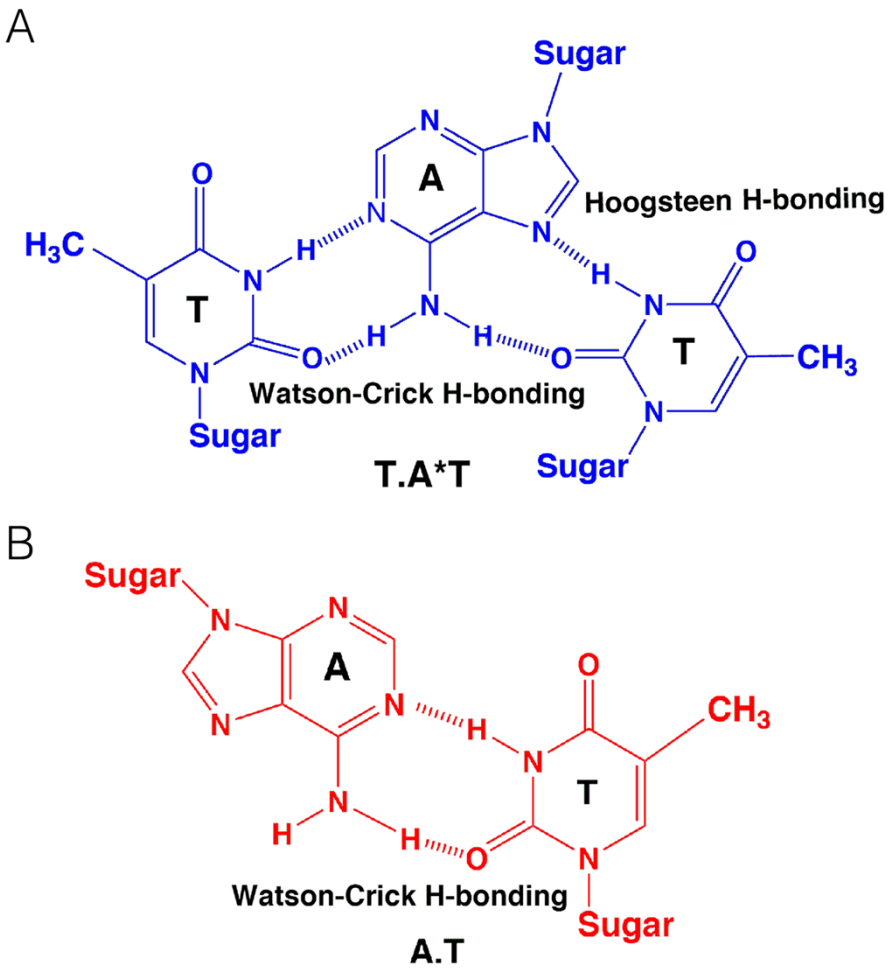

Fig. S1 Base pairing scheme in (A) triplex (T.A*T) and (B) duplex (A.T) DNA.

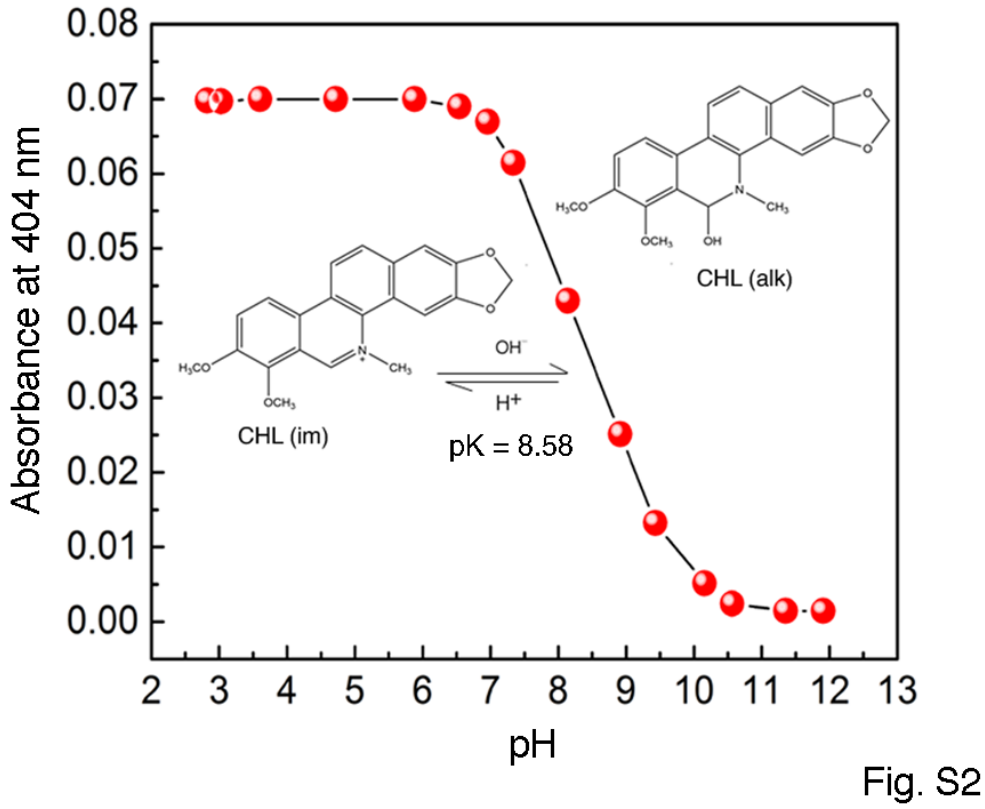

Fig. S2 pH dependent equilibrium between iminium and alkanolamine forms of Chelerythrine (CHL).

Experimental methods

UV-visible absorption spectrophotometric analysis

UV-visible absorbance studies were performed using a matched pair of quartz cells with a 1 cm path length and were recorded in a Shimadzu UV-1900i spectrophotometer (Shimadzu Corporation, Japan). It was equipped with a temperature controller (TCC-CONTROLLER, Shimadzu) to maintain constant temperature of both the sample and reference cells using Peltier effect. During the UV-Vis absorption spectrophotometric titrations, a known concentration of CHL solution was kept in the sample cell while buffer solution of equal volume was kept in reference cell. Now increasing concentration of nucleic acids (DNA triplex or duplex) was introduced to both the sample and reference cells. The solutions were stirred well after each addition of the aliquot and given sufficient times to equilibrate before recording data. To avoid the possibility of aggregation and to prevent adsorption to the walls of the cuvette, the absorbance values were kept at minimum possible values.

Fluorescence spectral analysis

Shimadzu RF-5301PC Spectrofluorimeter (Shimadzu Corporation, Kyoto, Japan) was employed for steady state fluorescence measurements. All the spectrofluorimetric experiments were carried out in a fluorescence free quartz cell of 1 cm path length. During the spectrofluorimetric titration, a fixed concentration of CHL was titrated against increasing concentration of both triple and double helical DNA structures. The fluorophore was excited at 400 nm, as at this wavelength, particularly the iminium form of CHL gets excited and alkanolamine form hardly shows any absorbance. Each fluorescence experiment was carried out with the excitation and emission band passes set at 5 nm and 10 nm respectively.

Analysis of binding data and evaluation of binding parameters

The data obtained from UV-visible absorption studies were cast into the following Benesi-Hildebrand equation for 1:1 stoichiometry to evaluate the binding parameters [1]

$$\frac{1}{\Delta A} = \frac{1}{\Delta A_{\max}} + \frac{1}{K_b \Delta A_{\max}} \frac{1}{[P]} \quad ----(S1)$$

Here $\Delta A_{\max} = | A_0 - A_\infty |$ and $\Delta A = | A_0 - A_x |$. A_0 , A_x and A_∞ are the absorbance of CHL in absence of any DNA polymer, at any intermediate concentration of triple/ double helices and at a concentration of complete saturation with DNA triplex /duplex forms respectively. [P] is the concentration of the DNA polymer and K_b depicts the binding constant for the complexation and it is obtained from the ratio of intercept to slope $\left(K_b = \frac{Intercept}{Slope} \right)$.

Likewise, the spectrofluorimetric data obtained from the titration of CHL with both forms of DNA triplex and duplex were cast into the following Benesi-Hildebrand equation for 1:1 stoichiometry to determine the binding parameters [1]

$$\frac{1}{\Delta F} = \frac{1}{\Delta F_{\max}} + \frac{1}{K_b \Delta F_{\max}} \frac{1}{[P]} \quad ----(S2)$$

Here again, $\Delta F_{\max} = | F_0 - F_\infty |$ and $\Delta F = | F_0 - F_x |$. F_0 , F_x and F_∞ are emission intensities of CHL in absence of polymer, at an intermediate concentration of polymer and at a concentration of complete saturation respectively. [P] is the concentration of the DNA polymers and K_b denotes the binding constant for the complexation and obtained from the ratio of intercept to slope (K_b=Intercept/Slope). For further clarification, the data were again

analysed by employing Benesi-Hildebrand equation for 1:2 stoichiometry of the following forms.[1]

$$\frac{1}{\Delta A} = \frac{1}{\Delta A_{\max}} + \frac{1}{K_b \Delta A_{\max}} \frac{1}{[P]^2} ----(S3)$$

$$\frac{1}{\Delta F} = \frac{1}{\Delta F_{\max}} + \frac{1}{K_b \Delta F_{\max}} \frac{1}{[P]^2} ----(S4)$$

Thermal melting analysis

Thermal melting analysis of both the triple and double helical forms of DNA in the absence and presence of the alkaloid, CHL was conducted by monitoring changes in the absorbance values at 260 nm with increasing temperature from 25 ℃ to 95 ℃ at a scan rate of 1℃/min by using the previously mentioned spectrophotometer associated with an accurate temperature controller (TMSPC-8i, Shimadzu Corporation, Japan). Before recording the absorbance values, the samples were given enough time to equilibrate at each temperature. The final presented data are the replicate of five measurements.

Fluorescence quenching analysis

The fluorescence quenching studies were carried out by employing an external anionic quencher, potassium iodide (KI). Solution of KNO_3 was mixed with KI at different proportions to maintain a fixed total ionic strength of the solution. In these quenching experiments, the fluorescence intensities at the emission maxima of CHL (573 nm) were monitored against the increasing concentration of KI for both free and DNA-bound CHL. The data were then plotted in the following form of Stern-Volmer equation [2]

$$\frac{F_0}{F} = 1 + K_{SV}[Q] ----(S5)$$

Where, F_0 and F are the fluorescence intensities in absence and presence of the quencher (KI) respectively and K_{SV} is the Stern-Volmer quenching constant. The magnitude of K_{SV} is indicative of the accessibility of the fluorophore CHL, to the anionic quencher, iodide (I^-). The slope of the F_0/F versus [KI] plot yields the value of K_{SV}. Presented data were an average of five measurements.

Fluorescence lifetime measurements

Time-correlated single-photon counting (TCSPC) method was employed to evaluate the excited state lifetime of CHL. Fluorescence decay of CHL was monitored in the absence and presence of increasing concentration of DNA triplex/duplex at an ambient temperature of 298.15 K in 310 mM cacodylate buffer of pH 6.50. During the experiments photo-excitation was done at 370 nm for CHL using a picosecond diode laser (DeltaFlex TCSPC system-PPD 800) and the fluorescence intensity was monitored at 573 nm for CHL. The fluorescence decay data were collected on a PMT detector (TBX-07C) and the time-dependent fluorescence intensity was analysed using the following equations [3]

$$F(t) = \sum_i \alpha_i \exp\left(-t / \tau_i\right) ----(S6)$$

Here α_i denotes the ith pre-exponential factor, τ_i refers to the decay time of ith component. The decay time is the lifetime of fluorophore in the excited state. For multi-exponential decay, the amplitude average lifetime $< \tau >$ was calculated using the following relations [3]

$$< \tau >= \sum_i a_i \tau_i ----(S7)$$

Where,
$$a_i = \frac{\alpha_i}{\sum_i \alpha_i} ----(S8)$$

Here, τ_i is the fluorescence lifetime and a_i is the normalized pre-exponential factor of ith decay component where i ranges from 1 to 3 for tri-exponential decay. The quality of the fitted decay profile was justified from the value of χ^2, which should range from 0.9 to 1.1.

Steady-state fluorescence polarisation anisotropy

Steady state fluorescence anisotropy (r) is an experimental measure of fluorescence depolarization, which is defined by the following equation proposed by Larsson *et. al.* [3,4]

$$r = \frac{I_{VV} - GI_{VH}}{I_{VV} + 2GI_{VH}} ----(S9)$$

Where G (G factor) is defined as the ratio of vertical to horizontal emission intensities while using the horizontally polarized excitation light $(G = I_{HV} / I_{HH})$. G-factor is related to the monochromator wavelength and slit widths. I_{VV} and I_{VH} correspond to the intensities obtained when the emission polarizer is oriented vertically and horizontally respectively while the

excitation light is polarized vertically. The fluorophore was excited at the wavelength of 400 nm and the emission intensity was monitored at 573 nm. Each presented data was an average of at least six measurements.

Time-resolved fluorescence polarisation anisotropy

Time-resolved fluorescence anisotropy studies were performed by employing time-correlated single-photon counting (TCSPC) method using the same instrumental arrangement as described in the fluorescence lifetime measurement study. The data were analysed using EzTime software as described earlier. The fluorescence anisotropy decay function can be represented by the following expression[3]

$$r(t) = \frac{I_{VV}(t) - GI_{VH}(t)}{I_{VV}(t) + 2GI_{VH}(t)} ----(S10)$$

Where, G, I_{VV} (t) and I_{VH} (t) have their usual respective meaning as described in steady-state fluorescence anisotropy method. Moreover, the bi-exponential and "dip-and-rise" fluorescence anisotropy decay patterns, observed for the fluorophore (CHL), while entrapped in DNA triplex and duplex-bound environment respectively, are explained using a series of mathematical functions, the detail of which are elucidated in the upcoming result and discussion segment.

Fluorescence contact energy transfer and determination of quantum efficiency

To demonstrate the energy transfer phenomenon occurring from DNA triplex/duplex to CHL, excitation spectra of CHL in the presence and absence of DNA bases were recorded in the wavelength range of 220- 310 nm by keeping the emission wavelength fixed at 573 nm. For further confirmation of the fluorescence energy transfer process, sensitized emission spectra were monitored in the wavelength region between 450 nm to 750 nm by exciting the samples at their respective excitation maxima. The efficiency of energy transfer from nucleic acid to the bound fluorophore was quantitatively measured throughout the wavelength range by using the following equation [5]

$$Q = \frac{q_b}{q_f} = \frac{I_b}{I_f} \times \frac{\varepsilon_f}{\varepsilon_b} ----(S11)$$

Where q_b and q_f are the quantum efficiencies of bound and free CHL respectively. I and ε represent the excitation intensity and molar extinction coefficient respectively. The

subscripts; b and f denote the nucleic acid bound and free state of the alkaloid, CHL, respectively. The ratio, Q_i/Q_{310} was plotted against excitation wavelength for both CHL-T. A*T and CHL-A. T systems. The normalization wavelength was chosen to be 310 nm as DNA hardly shows any absorbance at this wavelength.

Competitive displacement assay

Competitive displacement assay experiments were conducted using a well-known and strong DNA intercalator, ethidium bromide (EtBr) (ε = 5680 M^{-1} cm^{-1}, λ_{ex} = 478 nm, and $\lambda_{max}^{em} \sim 620$ nm.[5,6] using the aforesaid spectrofluorimeter (Shimadzu RF-5301PC Spectrofluorimeter, Shimadzu Corporation, Kyoto, Japan) at an ambient temperature of 298.15 K. A solution of CHL and DNA polymers (T.A*T/ A.T) at a ratio of 1:30 was titrated against EtBr. The entire experiment was done by exciting the system at 400 nm. Excitation wavelength was so chosen because at this wavelength both CHL and EtBr can be excited simultaneously and the emission response can be monitored properly in the course of this displacement phenomenon.

Spectropolarimetric studies: circular dichroism spectral analysis

Circular dichroism (CD) studies on T.A*T and A.T in the absence and presence of the increasing concentration of CHL were carried out by JASCO J815 spectropolarimeter (JASCO International Co., Japan), equipped with a temperature controller and a thermal programmer (model PFD 425L/15). A fixed scanning speed of 100 nm/min was kept throughout the recordings of all the CD spectra within the wavelength between 200 nm and 450 nm. The final CD spectra were obtained from an average of five scans and smoothed to enhance the signal-to-noise ratio. They were further converted in terms of molar ellipticity ([θ], in units of deg cm^2 $dmol^{-1}$) using the software provided with the spectropolarimeter and adjusted based on the nucleic acid-polymer concentration. The final presented data are the average of three scans.

Evaluation of thermodynamic parameters

To get an insight into binding forces involved in the complexation of CHL with DNA triplex (T.A*T) and duplex (A.T) forms, thermodynamic parameters were evaluated using the fluorescence spectrofluorimetric titration, performed at three different temperatures i.e., 290.15, 300.15 and 310.15 K. The spectral data were then used to calculate the binding constants by employing Benesi-Hildebrand equation (for 1:1 stoichiometry) as mentioned earlier. The experimental data were cast into van't Hoff plot (ln K_b vs. 1/T) and from the

slope we obtained the standard molar enthalpy change (ΔH°), which was considered to be constant within our experimental temperature window.

$$\frac{\partial \ln K_b}{\partial \ln (1/T)} = -\frac{\Delta H^0}{R} ----(S12)$$

The standard molar Gibb free energy change (ΔG°) was obtained using the following relation:

$$\Delta G^0 = -RT \ln K_b ----(S13)$$

For each temperature, standard molar entropy change (Δ S°) was calculated by the following equation:

$$\Delta S^0 = \frac{\Delta H^0 - \Delta G^0}{T} ----(S14)$$

Theoretical study

The photophysical properties of CHL was again explored theoretically and all the computations have been performed using the density-functional-theory (DFT)[7] and time-dependent DFT (TDDFT)[8-12] methods with Becke's three-parameter hybrid exchange function with the Lee-Yang-Parr gradient-corrected correlation functional (B3LYP)[13–15] as well as the 6-311+G (d, p) basis set as incorporated in the Gaussian 16 suite of programs.[16]The ground state (S_0) geometry optimization of CHL was executed in the gas phase at the B3LYP/6-311+G (d, p) level of theory. Further, the gas-phase-optimized structure was utilized for the optimization of the geometry with water as a solvent, at the same level of theory in the framework of the CPCM [17-19]model. The latter geometries were used to perform the geometry optimization of the first excited singlet state (S_1) utilizing the same level of theory. Further, to confirm that the structures should correspond to the energy minima, harmonic vibrational frequencies were evaluated for the optimized geometries for all S_0 and S_1 states. Moreover, the geometries of S_0 and S_1 states were optimized without constrain of bonds, angles and dihedral angles. The calculation of vertical excitation energy was also performed from the ground-optimized structure based on TDDFT methodology with CPCM using B3LYP/6-311+G (d, p) level of theory. Lastly, Gauss View program[20] was used for visualization of the studied system.

Preparation of T.A*T triplex followed by its characterization

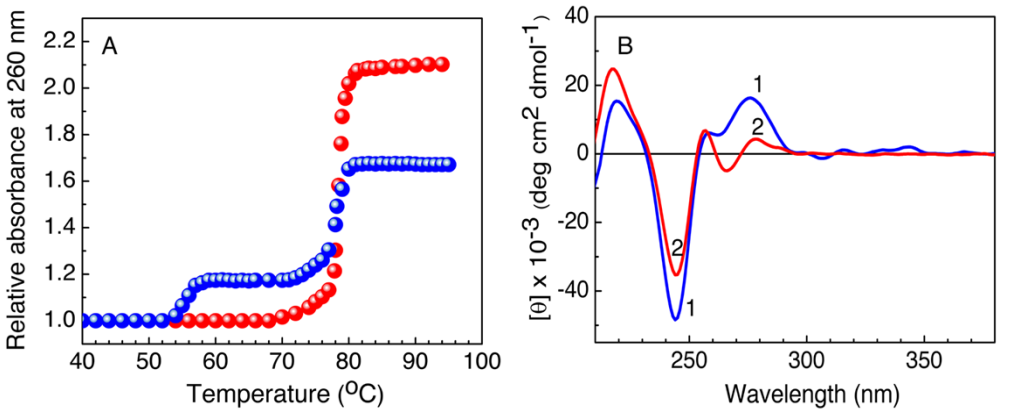

Fig. S3

Fig. S3 (A) Thermal melting profiles of T.A*T triplex (blue circles) and A.T duplex (red circles) in 310 mM cacodylate buffer of pH 6.50. (B) Characteristic circular dichroic spectra of T.A*T triplex (25 µM, curve 1) and A.T duplex (25 µM, curve 2) in 310 mM cacodylate buffer of pH 6.50 at 298.15 K.

DNA triplex, T.A*T was prepared by following the method, reported in previous data.[21] Poly (dT) (hereafter T) and poly (dA). poly(dT) (A.T) were mixed in equimolar ratio (1:1 molar) in 310 mM cacodylate buffer of pH 6.50 and the mixture was heated up to 90 °C for at least 30 min for the complete denaturation of the duplex strands. Then, to ensure the renaturation process, the resulting mixture was kept to cool down slowly at a rate of 0.5 °C/min to attain room temperature and it was further kept at 4°C overnight. The formation of T.A*T triplex was confirmed through characterization by thermal melting and CD spectral studies (Fig. S3). The characteristic melting profiles of DNA triplex and duplex [21,22] are represented in Fig. S3A. The melting profile of triplex displayed two different transition temperatures. The first transition occurred at ~ 55.8 °C (T_{m1}) whereas the second transition took place at ~ 78.2 °C (T_{m2}). The first transition indicates the detachment of the Hoogsteen base-paired strand whereas the second transition is indicative of the dissociation of the Watson-Crick base-paired strand into single strands. The thermal melting temperature (T_m) of parent duplex (A.T) was found to be around 78.5 °C. Thus, the occurrence of two different characteristic thermal melting profile for T.A*T triplex and A.T duplex, as well as the resemblance of the second melting temperature (T_{m2}) of T.A*T to the melting temperature of the parent duplex, ensures the formation of the triplex structure.

The CD spectra of DNA triplex and the corresponding parent duplex are shown in Fig. S3B. In the CD spectra the T.A*T triplex showed two characteristic positive bands at around 219

nm and 275 nm respectively followed by a hump at ~257nm and also a large negative band around 244 nm. Whereas the A.T duplex was characterized by a positive band ~217 nm and two small positive bands around 256 nm and 278 nm respectively associated with two negative bands around 244 nm and 265 nm respectively. Hence the representative CD spectra were remarkably different from each other, which in turn, again confirm DNA triplex formation. Moreover, both the CD spectra characterizing DNA triplex (T.A*T) and duplex (A.T) matched well with previously reported studies. [4,21,22]

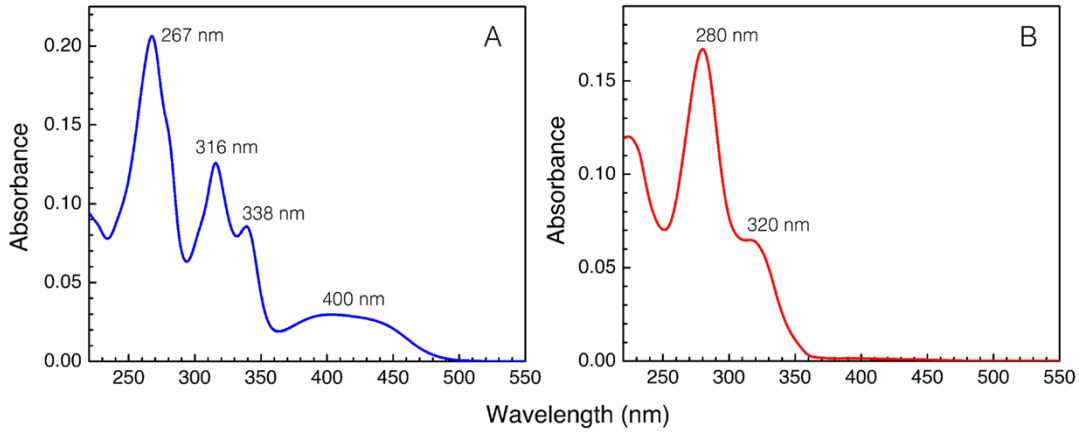

Fig. S4

Fig. S4 Absorption spectra of (A) iminium (3.53 µM) form of CHL in 10 mM CP buffer of pH 6.50 at 298.15 K and (B) alkanolamine (3.53 µM) form of CHL in 10 mM CBC buffer of pH 10.30 at 298.15 K.

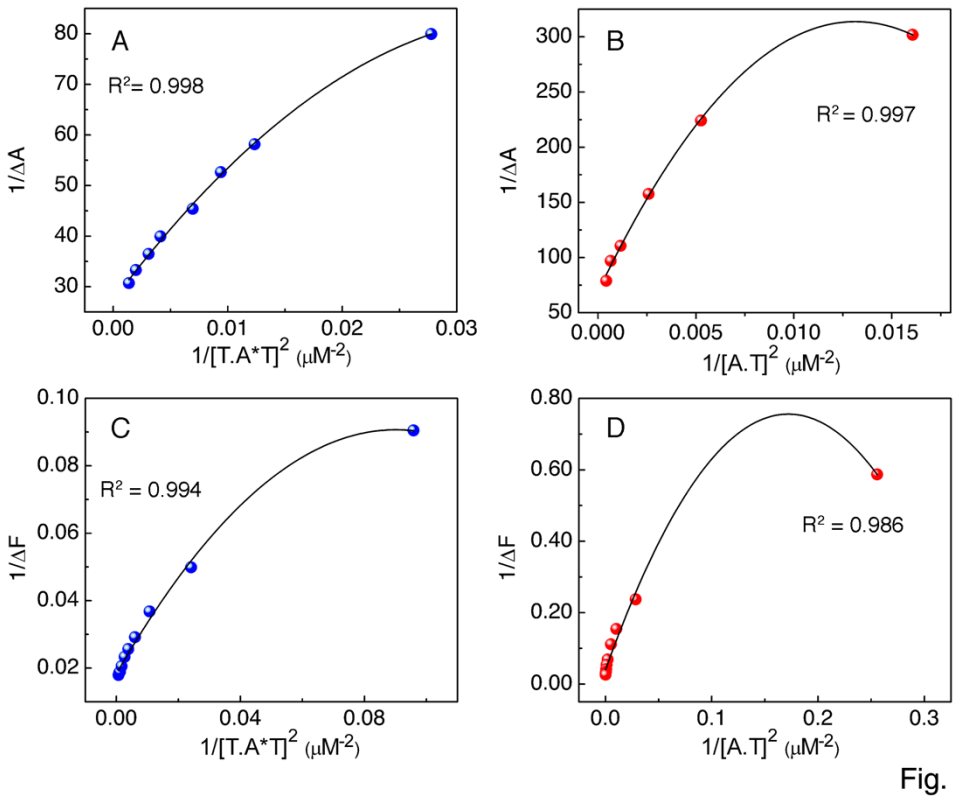

Fig. S5

Fig. S5 Benesi-Hildebrand plot for 1:2 stoichiometry obtained from UV-visible spectrophotometric titration for the binding of CHL with T.A*T (panel A) and A.T (panel B). Benesi-Hildebrand plot for 1:2 stoichiometry obtained from spectrofluorimetric titration for the binding of CHL with T.A*T (panel C) and A.T (panel D) in 310 mM cacodylate buffer of pH 6.50 at 293.15 K. The corresponding solid curves are the polynomial best fit of the experimental points.

Mode of binding: fluorescence quenching study

The quenching ability of a given quencher molecule alters depending on the binding location of the fluorophore whether it resides along the groove or intercalates within the base pairs/triplets of a given nucleic acid structure. Intercalatively bound fluorophores are in much more confined environment, away from the external quencher as compared to those which are bound to the nucleic acid through groove binding mode. Stern-Volmer quenching constant (K_{SV}) gives a quantitative measure to the quenching capabilities of quencher. Greater the value of K_{SV}, stronger is the efficiency of quenching. Here we have used potassium iodide (KI), more precisely, iodide (I^-) as an anionic quencher. The negative charge on the phosphate backbones of T.A*T and A.T produces an electrostatic repulsion to the anionic quencher, iodide and thus restricts the insertion of the quencher into the interior core of the

helix. As a result, in interactively bound condition, quencher will not be able to quench the fluorophore emission with that much efficiency as compared to its free form. Hence K_{SV} value should diminish compared to its free form more prominently when the fluorophore resides deeper inside the helix of nucleic acid compared to the groove bound situation with reference to the free fluorophore in bulk aqueous medium.[2]In fact, the fluorophore which binds to the groove of nucleic acid, exhibits the K_{SV} value close to that of free fluorophore. For our present study, the Stern-Volmer plots for quenching experiment are presented in Fig. S6. Quenching constants (K_{SV}) for free, duplex-bound, and triplex-bound CHL are 9.27, 7.98 and 5.04 M^{-1} respectively. The sufficient reduction in K_{SV} values indicate that CHL binds to both the forms of DNA polymers in intercalative mode. Again, stronger reduction of K_{SV} in case of triplex-bound CHL than that in the corresponding duplex-bound form conveys a greater extent of intercalative penetration of CHL in the triplex-bound environment. [2,4,23]

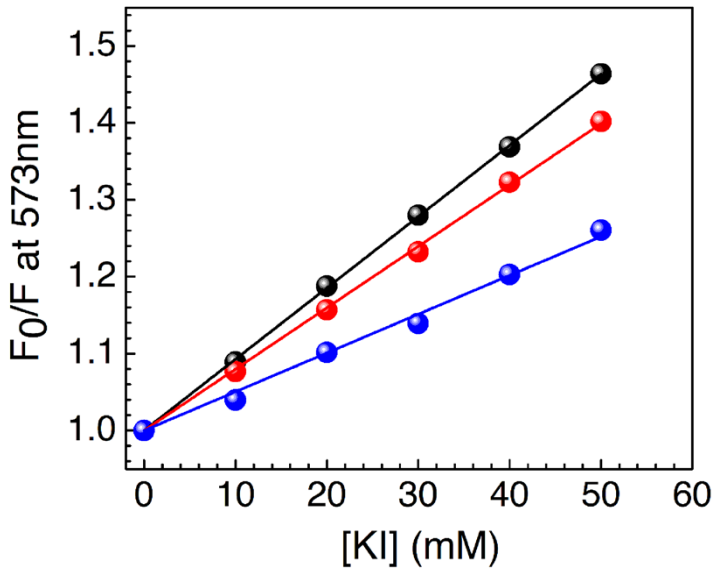

Fig. S6

Fig. S6 Stern-Volmer plots for the fluorescence quenching of CHL by KI in the absence (black circles) and in the presence of T.A*T triplex (blue circles) and A.T duplex (red circles) in 310 mM cacodylate buffer of pH 6.50 at 298.15 K.

Steady-state fluorescence anisotropy study

In absence of any sort of complexation with biopolymers, free fluorescent probe exerts an unrestricted tumbling motion resulting into quick depolarization of emission radiation and thereby leading to low fluorescence anisotropy. Whereas, association with bio-macromolecules or bio-mimetic heterogeneous moiety such as nucleic acids, proteins, lipids,

cyclodextrins, micelles etc., leads to confinement of the fluorophore into a rigid environment resulting in curbing the rotational motion and thereby increasing the anisotropy value by restricting fast depolarization. Thus, anisotropy value implies the extent of rigidity in the direct surrounding of fluorophore of interest. For our present study, the variation of steady state fluorescence anisotropy of CHL as a function of concentration of DNA polymers is presented in Fig. S7. Initially, in absence of any polymer, CHL exhibits a very low anisotropy value of 0.031, then with gradually increasing the concentration of DNA polymers, the anisotropy value shows a steep rise pattern, indicating the occurrence of motional restriction on the probe due to entering into the restricted environment within DNA-heterogeneous environment from free aqueous medium. Further addition of DNA polymers leads the anisotropy value reaching to a plateau region, probably making a sense of attaining the saturation in interaction between the probe and DNA polymers. These saturation anisotropy values were found to be 0.076 and 0.113 for duplex (A.T) and triplex (T.A*T) bound CHL respectively. As in steady-state anisotropy, we usually monitor at the emission maxima of the fluorophore (CHL), therefore, the obtained anisotropy outcome would mainly reflect the motional restriction, imposed on the fluorophore as an impact of complexation with the polymers. Hence, a considerable enhancement of the anisotropy value in the saturation region reflects the fact that CHL molecules are experiencing substantial degree of motional restriction while entrapped within the rigid DNA environment compared to that in the free aqueous buffer solution.[2,23-25]Comparatively higher extent of alteration in the anisotropy value was observed in case of triplex bound CHL compared to the duplex bound state. This higher fluorescence anisotropy of triplex-bound CHL compared to duplex-bound CHL may also originate from the slower global tumbling of the larger triplex polymer than that of the duplex form. Actually, both these factors can contribute to the enhanced fluorescence anisotropy values. Thus, our experimental observation suggested that possibly a greater amount of restriction was imposed on the rotational motion of CHL molecules in the triplex-bound environment than that in the duplex-bound state, indicating a probability of stronger intercalation of CHL within T.A*T than A.T. Further support for stronger intercalation of CHL within triplex compared to the duplex form is discussed in the upcoming results and discussion sections (main manuscript).

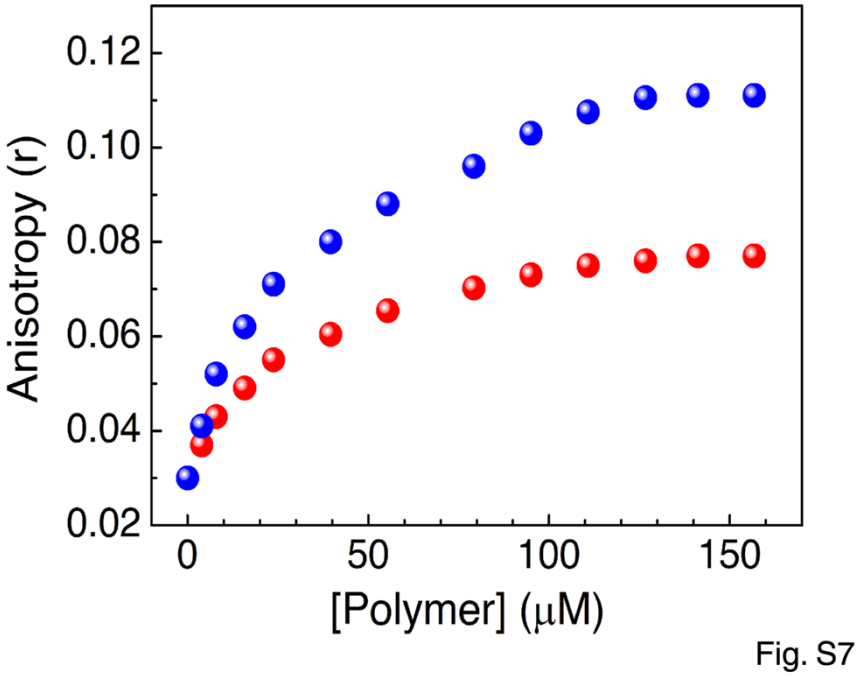

Fig. S7 The variation of steady state fluorescence anisotropy (r) of CHL plotted as a function of concentration of T.A*T triplex (blue circles) and A.T duplex (red circles). Each data point is an average of 10 individual measurements. λ_{ex} and λ_{em} for CHL 400 nm and 573 nm, respectively.

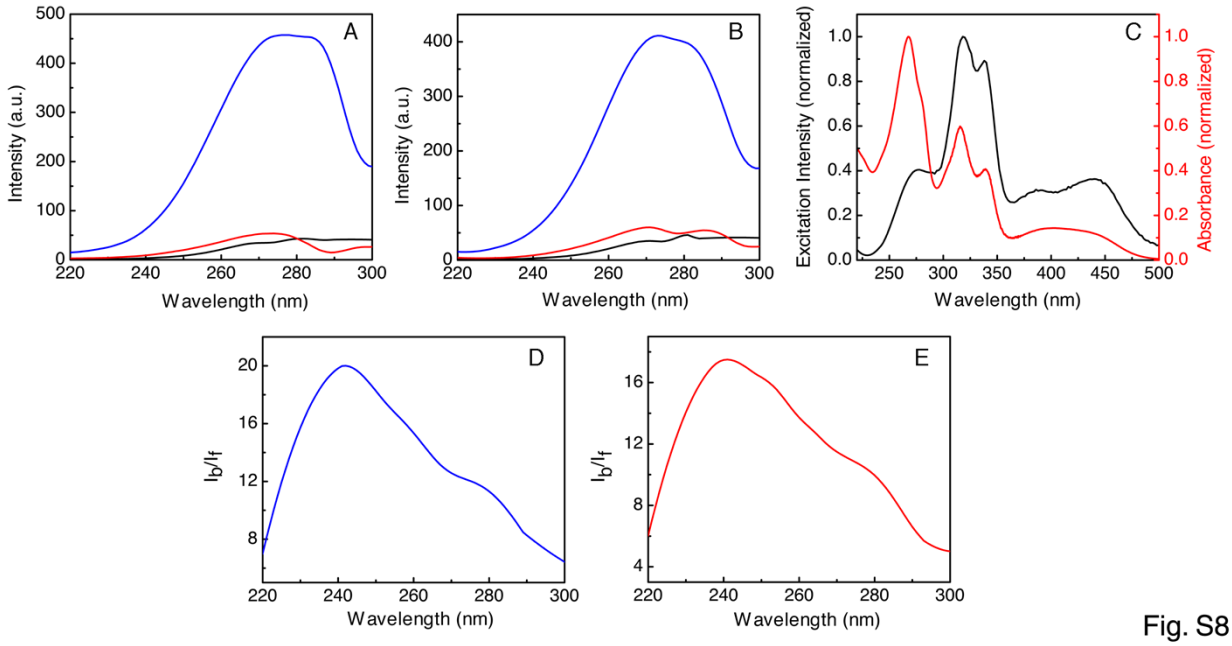

Fig. S8

Fig. S8 Fluorescence excitation spectra of (A) T.A*T triplex (red curve), CHL in absence (black curve), and presence (blue curve) of T.A*T triplex and (B) A.T duplex (red curve), CHL in absence (black curve), and presence (blue curve) of A.T duplex while keeping the emission wavelength at 573 nm. (C) Normalized fluorescence excitation spectra of CHL (black curve) and normalized absorption spectra of CHL (red curve). (D) Ratio of excitation of T.A*T-bound CHL to that of free CHL at emission wavelength of λ_{em} = 573 nm. (E) Ratio of excitation of A.T-bound CHL to that of free CHL at emission wavelength of λ_{em} = 573 nm. All the spectra and data are collected in 310 mM cacodylate buffer of pH 6.50 at 298.15 K.

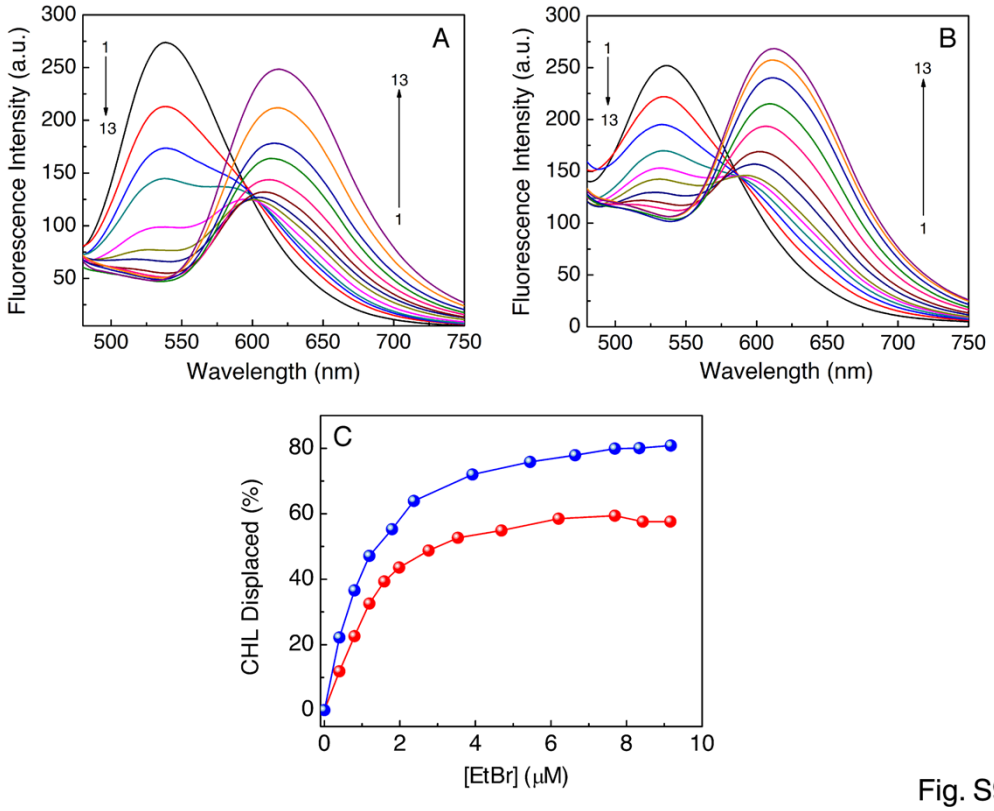

Fig. S9

Fig. S9 Competitive displacement assays using fluorescence spectroscopy. (A) Fluorescence spectra of CHL-T.A*T triplex complex with increasing concentration of EtBr and (B) Fluorescence spectra of CHL-A.T duplex complex with increasing concentration of EtBr. (C) Percentage displacement of CHL from T.A*T (blue circles) and A.T (red circles) environment as a function of EtBr concentration at emission wavelength of 540 nm. All the spectra are collected in 310 mM cacodylate buffer of pH 6.50 at 298.15 K.

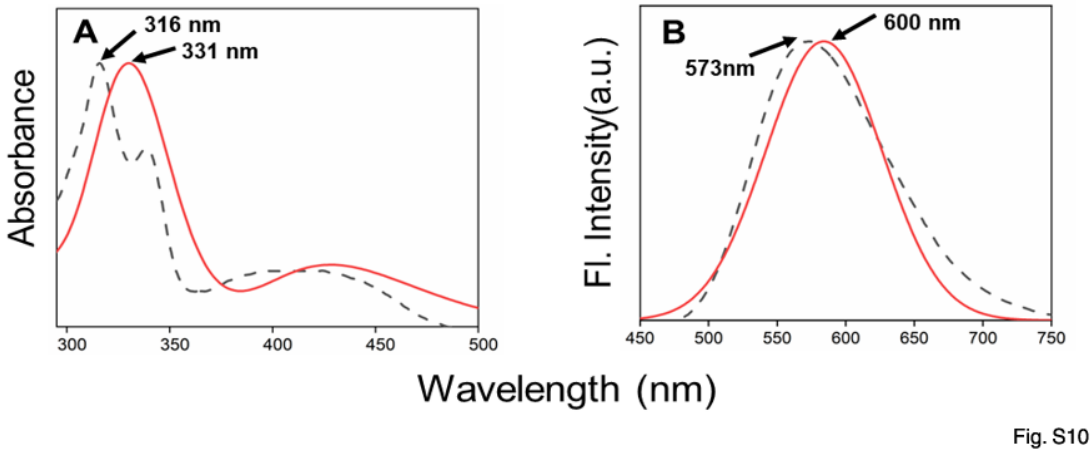

Fig. S10 Theoretical (red line) and the corresponding experimental spectra (dashed line) for CHL- (A) Absorption (at full width at half maxima (fwhm) = 100 nm and (B) Fluorescence (fwhm = 100 nm).

References:

1 H. A. Benesi and J.H. Hildebrand, *J. Am. Chem. Soc.*, 1949, **71**, 2703-2707.

2 J. R. Lakowicz, *Principles of Fluorescence Spectroscopy, Plenum Press*, U.S.A, New York, 2006.

3 A. Larson, C. Carlsson, M. Jonsson and B. Albinsson, *J. Am. Chem. Soc.,* 1994, **116**, 8459-8465.

4 P. V. Scaria and R.H. Shafer, *J. Biol. Chem*., 1991, **266**, 5417-5423.

5 J. B. LePecq and C. Paoletti, *J Mol Biol*., 1967, **27**, 87-106.

6 N. C. Garbett, N. B. Hammond and D. E. Graves, *Biophys. J*., 2004, **87**, 3974–3981.

7 W. Kohn, *Rev. Mod. Phys*., 1999, **71**, 1253.

8 E. Runge and E. K. U. Gross, *Phys. Rev. Lett*., 1984, **52**, 997.

9 P. Salek, O. Vahtras, T. Helgaker and H. Ågren, J. *Chem. Phys*., 2002, **117**, 9630.

10 F. Furche and R. Ahlrichs, *J. Chem. Phys*., 2002, **117**, 7433.

11 C. Ma, Y. Liu, C. Li and Y. Yang, *RSC Adv*., 2017, **7**, 13561-13569.

12 J. Zhao and Y. Yang, *J. Mol. Liq*., 2016, **220**, 735.

13 C. Lee, W. Yang and R. Parr, *Phys. Rev. B*, 1988, **37**, 785–789.

14 B. Miehlich, A. Savin, H. Stoll and H. Preuss, Chem. *Phys. Lett*., 1989, **157**, 200.

15 W. Kolth, A. Becke and R. Parr, *J. Phys. Chem*., 1990, **100**, 12974.

16 M.J. Frisch, G.W. Trucks, H. B. Schlegel, G. E. Scuseria, M.A. Robb, J. R. Cheeseman, G. Scalmani, V. Barone, G.A Petersson and H. Nakatsuji, Gaussian *16, Revision B.01, Gaussian, Inc*., Wallingford CT, 2016.

17 J. Tomasi, B. Mennucci and R. Cammi, *Chem. Rev.*, 2005, **105**, 2999.

18 R. E. Skyner, J. L. McDonagh, C. R. Groom, T. V. Mourik and J. B. O. Mitchell, *Phys. Chem. Chem. Phys*., 2015, **17**, 6174.

19 Y. Takano and K. N. Houk, *J. Chem. Theory Comput*., 2005, **1**, 70.

20 R. Dennington, T. A. Keith and J. M. Millam, *Gauss View, Version 6, Semichem Inc*., Shawnee Mission, KS, 2016.

21 A. Ray, G. S. Kumar, S. Das and M. Maiti, *Biochemistry*, 1999, **38**, 6239-6247.

22 S. Das, G. S. Kumar, A. Ray and M. Maiti*, J. Biomol. Struct. Dyn.*, 2003, **20**, 703-714.

23 S. Bhuiya, L. Haque, R. Goswami and S. Das, *J. Phys. Chem. B*, 2017, **121**, 11037-11052.

24 L. Haque, S. Bhuiya, R. Tiwari, A. B. Pradhan and S. Das, *RSC Adv.*, 2016, **6,** 83551−83562.

25 R. Goswami, L. Paul, H. Das, A. Ghosh, S. Chowdhury and S. Das, *J. Phys. Chem. B*, 2025, **129**, 9068-9082.